Thermodynamic Properties of *trans*-1,3,3,3-tetrafluoropropene [R1234ze(E)]: Measurements of Density and Vapor Pressure and a Comprehensive Equation of State‡

Mark O. McLinden[1]*, Monika Thol[1,2], Eric W. Lemmon[1]

[1]Thermophysical Properties Division, National Institute of Standards and Technology
325 Broadway, Boulder, CO 80305-3337 USA
tel: 1-303-497-3580; fax: 1-303-497-5224; markm@boulder.nist.gov

[2]present address: Lehrstuhl für Thermodynamik, Ruhr-Universität Bochum, Germany

*Corresponding Author

ABSTRACT

The thermodynamic properties of a hydrofluoro-olefin (HFO) refrigerant are presented. The p-ρ-T behavior of high-purity (99.993 %) R1234ze(E) was measured from 240 K to 420 K with pressures to 15 MPa by use of a two-sinker densimeter. The measurements extend from low-density vapor to compressed-liquid states. Vapor pressures were measured in the densimeter from 261 K to 380 K. The equation of state (EOS) for R1234ze(E) is expressed in terms of the Helmholtz energy as a function of temperature and density, and it is valid over the entire fluid surface. The formulation can be used for the calculation of all thermodynamic properties. Comparisons to experimental data are given to establish the accuracy of the EOS.

1. INTRODUCTION

R1234ze(E) or *trans*-1,3,3,3-tetrafluoroprop-1-ene is a fluorinated analogue of propene (propylene). The carbon-carbon double bond makes it unstable in the atmosphere, resulting in an atmospheric lifetime of only 0.05 years and a greenhouse warming potential (GWP) of 6 relative to CO_2 on a 100-year time horizon (Grebenkov *et al*., 2009). It is currently in limited commercial production and is used as a foam-blowing agent in applications requiring a low GWP. It is also of interest as a refrigerant.

In this work we present measurements of the thermodynamic properties of R1234ze(E). These data were used to develop a fundamental equation of state that is valid over the entire fluid surface and that can be used to calculate all of the thermodynamic properties. Our data are compared to the very limited literature data available for this fluid. Knowledge of the thermophysical properties is essential for the evaluation of refrigerants and the design of equipment using them. The present equation of state is compatible with the NIST REFPROP database (Lemmon *et al*., 2007), and it will be valuable in design studies of refrigeration systems using R1234ze(E). It must, however, be considered an interim property formulation; it will be updated as additional experimental data become available.

2. EXPERIMENTAL

2.1 Experimental Sample

The experimental sample of R1234ze(E) was provided by Honeywell International.§ The supplier's analysis indicated a purity of 99.993 %. The sample was degassed by freezing in liquid nitrogen, evacuating the vapor space, and thawing. The pressure over the frozen material on the fourth and final freeze-pump-thaw cycle was 1×10^{-4} Pa. We recovered the samples following the measurements and checked the purity by gas chromatography combined with mass spectrometric identification. No impurities or decomposition products were found.

---

§ Certain trade names and products are identified only to adequately document the experimental materials and procedure. This does not constitute recommendation or endorsement of these products by the National Institute of Standards and Technology, nor does it imply that the products are necessarily the best available for the purpose.

The presence of the double bond offers the possibility that R1234ze(E) could polymerize. To check for this (so as to avoid the formation of polymer inside our instruments), a high-pressure stainless steel test reactor was partially filled with liquid R1234ze(E) at room temperature and then heated to 445 K. Coupons of type 316 stainless steel, titanium, tantalum, beryllium copper, and gold-plated copper were also loaded into the reactor before sealing it. Based on the filling density, a pressure estimated at 20 MPa was generated. Upon opening the reactor, a very small quantity (< 1 mg) of a white, waxy solid, presumed to be a polymerization product of R1234ze(E), was found. These conditions were far in excess of any temperatures and pressures expected in a refrigeration system, but they served to advise us on the maximum temperatures and pressures for our measurements.

2.2 *p*-ρ-*T* Behavior

The present measurements utilized a two-sinker densimeter with a magnetic suspension coupling. This type of instrument applies the Archimedes (buoyancy) principle to provide an absolute determination of the density. This instrument is described in detail by McLinden and Lösch-Will (2007). Briefly, two sinkers of nearly the same mass and surface area, but very different volumes, are weighed separately with a high-precision balance while they are immersed in a fluid of unknown density. The fluid density ρ is given by

$$\rho = \frac{(m_1 - m_2) - (W_1 - W_2)}{(V_1 - V_2)} \ , \tag{1}$$

where m and V are the sinker mass and volume, W is the balance reading, and the subscripts refer to the two sinkers. Each sinker had a mass of 60 g; one was made of tantalum and the other of titanium. A magnetic suspension coupling transmitted the gravity and buoyancy forces on the sinkers to the balance, thus isolating the fluid sample from the balance. In addition to the sinkers, two calibration masses were also weighed. This provided a calibration of the balance and also the information needed to correct for magnetic effects as described by McLinden *et al.* (2007); these effects are quantified by a "coupling factor" ϕ, which is a measure of the effectiveness of the magnetic coupling. The coupling factor is nearly unity for this apparatus, but it also varies with the fluid; for the present measurements it varied from 1.000 021 in vacuum to 0.999 977 for R1234ze(E) at the highest measured density.

The temperature was measured with a 25 Ω standard platinum resistance thermometer (SPRT) and resistance bridge referenced to a thermostatted standard resistor. Pressures were measured with one of three vibrating-quartz-crystal type pressure transducers having full-scale pressure ranges of 2.8 MPa, 14.8 MPa, and 68.9 MPa. The transducer and pressure manifold were thermostatted at 313 K to minimize the effects of variations in laboratory temperature.

Measurements were carried out with three separate fillings of R1234ze(E) in the vapor, liquid, and extended critical regions. Typically, five replicate density determinations were made at each (T, p) state point. A total of 671 *p*-ρ-*T* data were measured at 136 (T, p) state points. Figure 1 depicts the points measured. The data are given in Table A1, where an average of the replicate points is reported. Measurements in vacuum were carried out before and after each filling to check the zero of the pressure transducers and the density zero of the densimeter.

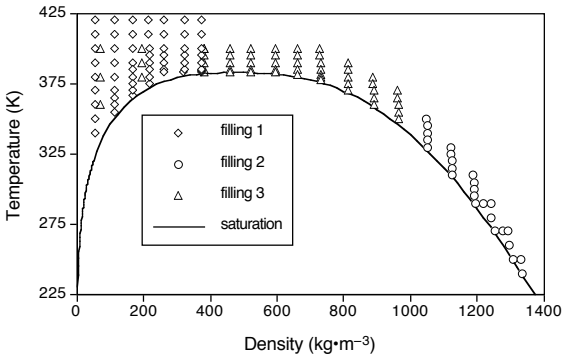

Figure 1. *p*-ρ-*T* points measured for R1234ze(E).

From the coupling factor ϕ and its variation with density it is possible to estimate the specific magnetic susceptibility of a fluid as detailed by McLinden *et al.* (2007). R1234ze(E) is slightly diamagnetic (as is typical for most fluids) with $\chi_s = -0.67 \times 10^{-8} \pm 0.12 \times 10^{-8}\ \mathrm{m^3 \cdot kg^{-1}}$.

A detailed uncertainty analysis for this instrument is provided by McLinden and Lösch-Will (2007) and McLinden and Splett (2008). Those results yield the expanded (k = 2, or approximately 95 % confidence level) uncertainty in the density:

$$\frac{u(\rho)}{\mathrm{kg \cdot m^{-3}}} = \left[\{56\}^2 + \{0.75 |(T/\mathrm{K} - 293)|\}^2 + \{1.25 p/\mathrm{MPa}\}^2 \right]^{0.5} \frac{10^{-6}\rho}{\mathrm{kg \cdot m^{-3}}} + 0.0014 \ . \tag{2}$$

The SPRT used to measure the temperature of the fluid was calibrated on ITS-90 from 83 K to 505 K by use of fixed-point cells (argon triple point, mercury triple point, water triple point, indium freezing point, and tin freezing

point). The expanded uncertainty in the temperature is 4 mK. The uncertainty of the pressure arises from three sources: the calibration of the transducers by use of a piston gage, the repeatability and drift of the transducers, and the uncertainty of the hydrostatic head correction. The expanded (k = 2) uncertainty of the pressure measurement is ($40 \times 10^{-6} \cdot p$ + 0.06 kPa) for the low-range transducer, ($40 \times 10^{-6} \cdot p$ + 0.30 kPa) for the mid-range transducer, and ($52 \times 10^{-6} \cdot p$ + 2.0 kPa) for the high-range transducer. To these must be added the uncertainty in the hydrostatic head correction, which amounted to 0.1 kPa for the compressed-liquid measurements and 0.2 kPa for the vapor-phase and supercritical measurements. The medium-range transducer was used for fillings 1 and 3, and the high-range transducer was used for filling 2.

For purposes of fitting an equation of state, it is customary to assume that the temperature and pressure (or sometimes temperature and density) are known exactly and to lump all uncertainties into a single value for the density (or pressure). This overall combined, or state-point, uncertainty is given by

$$u_C(\rho) = \left\{ \left[u(\rho) \right]^2 + \left[\left(\partial \rho / \partial p \right)_T u(p) \right]^2 + \left[\left(\partial \rho / \partial T \right)_p u(T) \right]^2 \right\}^{0.5} , \tag{3}$$

where u_C designates the combined uncertainty, the u are the individual uncertainties, and the derivatives are evaluated from an equation of state.

2.3 Vapor Pressure

Vapor pressures were measured by partially filling the densimeter cell with liquid and using it as a static vapor pressure instrument as described by McLinden (2009) (densities were not measured for these tests). Vapor pressures were determined at 28 temperatures from 261 K to 380 K. Five to eight replicate determinations were carried out at each temperature to yield 216 p_{sat} data. Table A2 reports an average of the replicates at each temperature. In addition to the main series of measurements (which were made on the first filling of R1234ze(E)), the vapor pressure was measured after completion of the vapor-phase p-ρ-T measurements and also after the liquid-phase p-ρ-T measurements to check for any possible sample degradation; these agreed with the earlier measurements within the uncertainty of the pressure measurement. The uncertainty in the vapor pressures is the transducer uncertainty given in Section 2.2 (the low-range transducer was used for $T \leq$ 340 K, and the medium-range transducer was used for $T \geq$ 345 K) plus a hydrostatic head uncertainty of 0.2 kPa for $T <$ 300 K, 0.35 kPa for 300 K < $T <$ 313 K, and 0.1 kPa for $T >$ 313 K.

3. EQUATION OF STATE

3.1 Pure-Fluid Model

The thermodynamic properties of R1234ze(E) are represented in terms of the reduced molar Helmholtz free energy A as a function of temperature T and density ρ. The equation is composed of separate parts arising from ideal-gas behavior (superscript *id*) and a "residual" or "real-fluid" (superscript *r*) contribution:

$$\alpha \equiv \frac{A}{RT} = \alpha^{id} + \alpha^{r} , \tag{4}$$

where R is the molar gas constant.

The "residual" or "real-fluid" contribution is given by

$$\alpha^{r} = \sum_{k=1}^{10} N_k \tau^{t_k} \delta^{d_k} \exp\left[-\delta^{l_k} \right] + \sum_{k=11}^{14} N_k \tau^{t_k} \delta^{d_k} \exp\left[-\eta_k \left(\delta - \varepsilon_k \right)^2 \right] \exp\left[-\beta_k \left(\tau - \gamma_k \right)^2 \right] , \tag{5}$$

where the temperature and density are expressed in terms of the dimensionless variables $\tau = T^*/T$ and $\delta = \rho/\rho^*$, where T^* and ρ^* are reducing parameters that are equal to the critical parameters. In this work we adopt the reducing temperature T^* = 382.52 K and density ρ^* = 489.23 kg·m^{-3} (4.29 mol·L^{-1}), which were found from the equation of state fit. These are in close agreement with the critical parameters reported by Higashi *et al.* (2010) of T_{crit} = 382.51 K and ρ_{crit} = 486 kg·m^{-3}; although the Higashi parameters were directly measured, adopting critical parameters from the fit maintains thermodynamic consistency between the critical parameters and the p-ρ-T data. The N_k are numerical coefficients fitted to experimental data. The first summation represents the more common form of the equation of state. The second summation represents the properties in the critical region; these terms go to zero away from the critical point. The parameters for Eq. (5) are given in Table 1.

Table 1. Parameters of the equation of state (Eq. 5).

k	N_k	t_k	d_k	l_k	η_k	β_k	γ_k	ε_k
1	0.0555630	1.00	4	0				
2	1.66927	0.34	1	0				
3	-2.53408	0.91	1	0				
4	-0.475075	1.23	2	0				
5	0.190055	0.46	3	0				
6	-1.25154	2.26	1	2				
7	-0.742195	2.50	3	2				
8	0.537902	2.00	2	1				
9	-0.741246	2.24	2	2				
10	-0.0355064	0.90	7	1				
11	1.58506	1.06	1	–	-1.02	-1.19	1.140	0.711
12	-0.502086	1.79	1	–	-1.34	-2.29	0.667	0.914
13	-0.191360	3.75	3	–	-1.08	-1.15	0.505	0.694
14	-0.975576	0.92	3	–	-6.41	-131.8	1.220	0.731

Table 2. Parameters of ideal-gas portion of the equation of state (Eq. 6).

k	a_k	b_k
1	5.8887	–
2	7.0804	620.
3	9.3371	1570.
4	2.5577	3953.

The ideal-gas contribution is represented as

$$\alpha^{\mathrm{id}} = \ln(\delta) + a_1 \ln(\tau) + \sum_{k=2}^{4} a_k \ln\left[1 - \exp(-b_k \tau)\right] , \tag{6}$$

and the parameters a_k and b_k are given in Table 2. The ideal-gas parameters were fitted to the ideal-gas heat capacity values of Hulse (2010), which were calculated from vibrational energies at the GGA/PW91/DND level of theory.

The equation of state was fitted to experimental data by use of nonlinear methods. All of the parameters and exponents were optimized for R1234ze(E) (as opposed to using an equation with fixed values of the exponents on temperature). In addition to optimizing the parameters to the data, numerous thermodynamic constraints were applied to ensure that the equation was well behaved and would reliably extrapolate beyond the range of the available data. These techniques enable a comprehensive equation of state with a relatively small number of terms. Nonlinear fitting requires starting values for all of the parameters and exponents, and we used a 14-term equation for propane as the starting point. The Helmholtz energy equation of state and the fitting process is described in detail by Lemmon *et al.* (2009); that paper also describes the calculation of all the thermodynamic properties from the Helmholtz energy.

3.2 Comparison to Experimental Data

The equation of state was fitted primarily to the present data because these are the most comprehensive and high-accuracy data presently available for R1234ze(E). Comparisons of the EOS with experimental vapor pressure data are given in Figure 2. The present data are

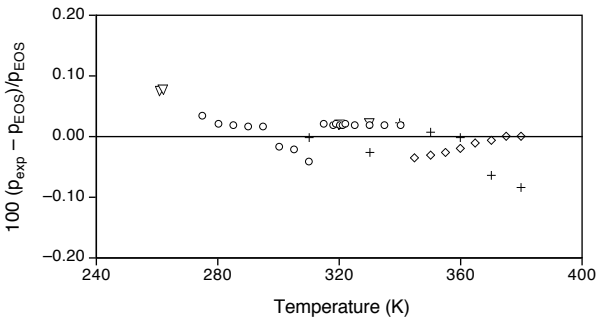

Figure 2. Relative deviations of the experimental vapor pressures for R1234ze(E) from the EOS; ○, present work, filling 1 using the low-range transducer; ◇, present work, filling 1 using the mid-range transducer; ▽, present work, filling 2 using the low-range pressure transducer; +, Tanaka *et al.* (2010a).

represented with a relative standard deviation of 0.028 %. The discontinuity in the data at a temperature of 313 K is due to larger uncertainties in the hydrostatic head correction as the pressure transducer transitions from vapor-filled to liquid-filled as the temperature is raised and the vapor pressure increases. The discontinuity at 345 K is due to the switch-over from the low-range pressure transducer to the mid-range pressure transducer, which has larger uncertainties. The vapor pressures of Tanaka *et al.* (2010a) are in excellent agreement with the present data and are represented with a relative standard deviation of 0.039 %. The data of Grebenkov *et al.* (2009) showed considerable scatter with a relative standard deviation of 1.78 %; they are not shown in the figure. Extrapolating the vapor pressure to the critical temperature yields a critical pressure p_{crit} = 3.6364 MPa.

Comparisons of the EOS with *p-ρ-T* data are given in Figure 3. The figure plots deviations in density for a given *(T, p)* state point except in the vicinity of the critical point ($0.6 \le \rho/\rho_{crit} < 1.6$) where comparisons are made in terms of deviations in the measured pressure compared with the pressures calculated with the EOS as a function of T and ρ. Because of the "flatness" of the isotherms near the critical point, comparisons of densities as a *f(T, p)* are less meaningful in this region. The present data are represented with a relative standard deviation of 0.032 %, and there are no obvious systematic trends with temperature, pressure, or density. The final three isochores of filling 3, at ρ = (381, 194, and 69) kg·m^{-3}, were near-replicates of three of the isochores measured with filling 1; the relative deviations differ by less than 0.015 %, indicating the excellent reproducibility of the densimeter and the stability of the sample.

The data of Tanaka *et al.* (2010a) are in excellent agreement with the present data at their lowest temperatures of 310 K and 320 K, but show increasing, systematic deviations as the temperature is increased. The relative standard deviation of the Tanaka *et al.* data is 0.087 %. The saturated-liquid density data of Grebenkov *et al.* (2010) were measured with standard density floats. They have a relative standard deviation of 0.22 %; the two points with deviations of –0.39 % and +0.41 % are plotted on the graph frame in Figure 3. The compressed-liquid and vapor-phase data of Grebenkov *et al.* (2010) were measured with a constant volume piezometer and show considerable scatter with relative standard deviations of 0.52 % and 1.31 %, respectively; they are not shown in the Figure.

The only directly-measured heat capacities presently available are the liquid-phase C_p data of Tanaka *et al.* (2010b). The deviations of these data are compared to the equation of state in Figure 4. These data have an uncertainty of 5 % and were not used in fitting the EOS. Nevertheless, they are generally represented within their uncertainty with a relative standard deviation of 2.16 %, but with a mean bias error of –1.51 %

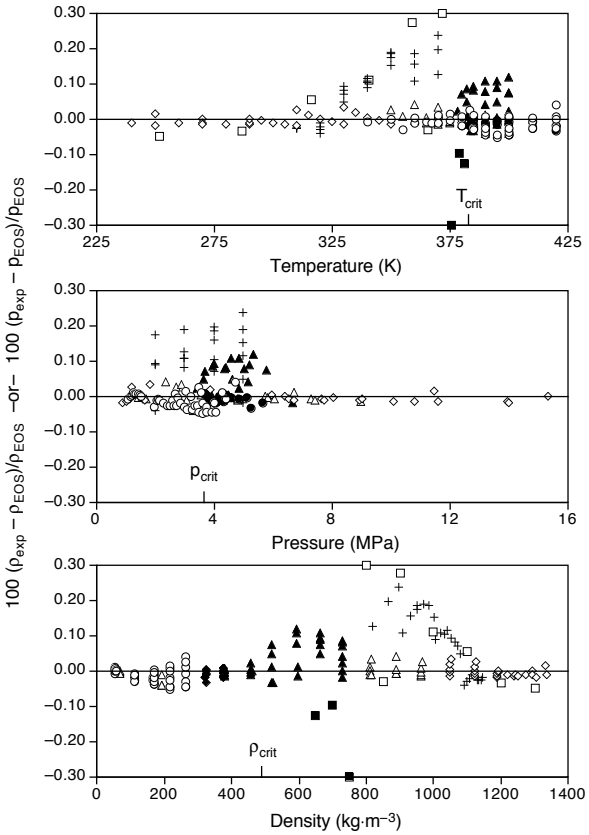

Figure 3. Relative deviations of the experimental *p-ρ-T* data for R1234ze(E) from values calculated with the equation of state; ○, present work, filling 1; ◇, present work, filling 2; △, present work, filling 3; +, Tanaka *et al.* (2010a); □, Grebenkov *et al.* (2009). The filled symbols indicate near-critical points where deviations in pressure are plotted; all other points are deviations in density.

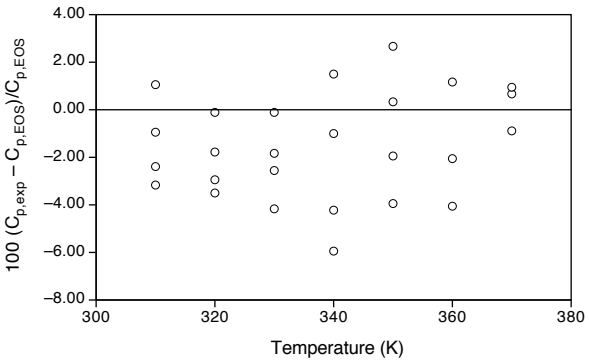

Figure 4. Relative deviations of the experimental heat capacities for R1234ze(E) from values calculated with the equation of state; ○, Tanaka *et al.* (2010b).

4. DISCUSSION AND CONCLUSIONS

We have presented comprehensive, high-accuracy measurements of the thermodynamic properties of R1234ze(E). The properties measured and their temperature and pressure ranges were selected to provide the data most essential for developing an accurate equation of state. The EOS based on these data, together with selected literature data, is the best currently available for this fluid and the best that is feasible given the currently available data. The EOS is entirely adequate to evaluate this fluid in typical refrigeration applications.

Further measurements would be warranted, especially if R1234ze(E) becomes widely used. Specifically, further caloric data in the liquid phase, such as accurate heat capacity and speed of sound data, would improve the representation of energy quantities, including enthalpy, entropy, and heat capacity. Speed of sound data in the vapor phase are needed to verify and improve the ideal-gas portion of the equation of state. No data are currently available below 240 K, and lower-temperature data would be desirable if low-temperature applications were anticipated for this fluid. Measurements at temperatures and pressures above the current data (420 K, 15 MPa) would require further investigation of the stability of R1234ze(E) with respect to thermal degradation and polymerization, but the present data should be adequate for most applications. The present work addressed only the thermodynamic properties and, at present, only Grebenkov *et al.* (2009) have published transport properties. Further measurements of the viscosity and thermal conductivity are also desirable.

REFERENCES

Grebenkov, A. J., Hulse, R., Pham, H., Singh, R., 2009, Physical properties and equation of state for trans-1,3,3,3-tetrafluoropropene. *3rd IIR Conference on Thermophysical Properties and Transfer Processes of Refrigerants*, Boulder, Colorado, International Institute of Refrigeration, paper no. 191.

Higashi, Y., Tanaka, K., 2010, Critical parameters and saturated densities in the critical region for trans-1,3,3,3-tetrafluoropropene (HFO-1234ze(E)). *J. Chem. Eng. Data,* 55: 1594-1597.

Hulse, R., 2010, Honeywell International, 20 Peabody St., Buffalo, NY 14210, personal communication.

Lemmon, E. W., Huber, M. L., McLinden, M. O., 2007, *NIST Standard Reference Database 23, NIST Reference Fluid Thermodynamic and Transport Properties—REFPROP, version 8.0*. Standard Reference Data Program, National Institute of Standards and Technology, Gaithersburg, MD.

Lemmon, E. W., Wagner, W.; McLinden, M. O., 2009,Thermodynamic properties of propane. III. Equation of state. *J. Chem. Eng. Data* 54: 3141-3180.

McLinden, M. O., 2009, Thermodynamic properties of propane. I. p-ρ-T behavior from 265 K to 500 K with pressures to 36 MPa. *J. Chem. Eng. Data,* 54: 3181-3191.

McLinden, M. O., Kleinrahm, R., Wagner, W., 2007, Force transmission errors in magnetic suspension densimeters. *Int. J. Thermophysics***,** 28: 429-448.

McLinden, M. O., Lösch-Will, C., 2007, Apparatus for wide-ranging, high-accuracy fluid (p-ρ-T) measurements based on a compact two-sinker densimeter. *J. Chem. Eng. Data,* 39: 507-530.

McLinden, M. O., Splett, J. D., 2008, A liquid density standard over wide ranges of temperature and pressure based on toluene. *J. Res. Natl. Inst. Stand. Technol.,* 113: 29-67.

Tanaka, K., Takahashi, G., Higashi, Y., 2010a, Measurements of the vapor pressures and $p\rho T$ properties for trans-1,3,3,3-tetrafluoropropene (HFO-1234ze(E)). *J. Chem. Eng. Data,* 10.1021/je900756g.

Tanaka, K., Takahashi, G., Higashi, Y., 2010b, Measurements of the isobaric specific heat capacities for trans-1,3,3,3-tetrafluoropropene (HFO-1234ze(E)) in the liquid phase. *J. Chem. Eng. Data,* 10.1021/je900799e.

ACKNOWLEDGMENTS

We thank Ryan Hulse and Rajiv Singh of Honeywell International for providing the high-purity sample of R1234ze(E). We thank Tara Lovestead of NIST for the chemical analysis of the sample.

APPENDIX—MEASURED DATA

Table A1. Experimental p-ρ-T data for R1234ze(E);
an average of the replicates at each temperature-pressure (T, p) state point is given.

T/K	p/MPa	ρ/(kg·m^{-3})	T/K	p/MPa	ρ/(kg·m^{-3})	T/K	p/MPa	ρ/(kg·m^{-3})
filling 1—vapor phase								
383.004	3.6548	375.243	400.000	4.078	263.456	420.001	3.6315	168.109
384.004	3.7117	375.336	410.000	4.4147	263.288	354.998	1.9727	113.760
385.004	3.7679	375.380	420.001	4.7443	263.089	359.998	2.0366	113.761
390.005	4.0449	375.718	374.996	3.0512	217.016	364.999	2.0991	113.748
395.005	4.3178	376.037	379.997	3.1961	217.246	369.999	2.1607	113.738
400.006	4.5878	376.173	384.998	3.3362	217.197	380.000	2.2812	113.700
410.007	5.1209	376.139	389.998	3.4733	217.122	390.000	2.3988	113.651
420.007	5.6474	375.960	394.998	3.6083	217.076	400.000	2.5138	113.580
382.998	3.6094	321.798	399.998	3.7410	216.976	410.001	2.6279	113.577
384.999	3.7065	323.618	409.999	4.0015	216.784	420.001	2.7395	113.518
389.999	3.9404	324.399	420.000	4.2572	216.646	339.998	1.0956	54.342
395.000	4.1698	324.863	366.995	2.6028	168.282	349.999	1.1478	54.427
400.000	4.3952	324.994	369.997	2.6673	168.481	360.000	1.1984	54.462
410.001	4.8377	324.936	374.998	2.7713	168.552	370.001	1.2504	54.608
420.002	5.2727	324.802	379.997	2.8724	168.530	380.002	1.3040	54.846
382.998	3.4813	263.494	384.998	2.9709	168.407	390.001	1.3573	55.074
384.998	3.5535	263.455	390.000	3.0687	168.374	400.002	1.4125	55.390
389.999	3.7306	263.271	400.000	3.2600	168.269	410.003	1.4681	55.707
395.000	3.9059	263.437	410.000	3.4471	168.159	420.003	1.5193	55.836
filling 2—compressed liquid								
240.002	1.6665	1335.09	289.996	7.7552	1219.27	319.994	6.4123	1123.58
249.999	11.4773	1331.95	289.997	1.2599	1193.11	324.994	9.0206	1122.67
250.001	0.9214	1307.05	294.993	4.4241	1191.71	329.995	11.6274	1121.82
259.999	6.5576	1295.49	299.996	7.6347	1190.61	329.995	1.8175	1051.78
269.998	15.3370	1292.92	304.995	10.8186	1189.50	334.994	3.8838	1050.92
269.999	8.9312	1276.18	309.995	14.0113	1188.52	339.995	5.9617	1050.15
270.000	1.0555	1252.19	309.995	1.1962	1125.58	344.995	8.0358	1049.36
279.997	6.7109	1243.08	314.994	3.8028	1124.54	350.001	10.1201	1048.66
289.996	13.9675	1240.05						
filling 3—compressed liquid and supercritical region								
350.000	2.7153	965.858	384.999	4.4230	730.984	400.000	5.0263	520.863
355.001	4.2741	965.035	389.998	5.1583	730.596	383.499	3.7039	460.389
360.001	5.8426	964.255	395.000	5.9063	730.192	384.999	3.8070	458.933
365.002	7.4173	963.498	400.001	6.6637	729.802	389.999	4.1498	458.743
370.002	8.9969	962.768	382.000	3.6734	664.097	394.999	4.4928	458.737
360.000	2.3773	891.030	385.000	4.0136	663.858	399.999	4.8362	458.687
365.001	3.5861	890.375	390.001	4.5995	663.581	400.000	4.6047	381.375
370.002	4.8109	889.740	395.001	5.2002	663.279	383.000	3.6568	380.483
375.003	6.0469	889.110	400.002	5.8111	662.950	385.000	3.7716	380.557
380.003	7.2912	888.486	382.999	3.6886	596.548	389.999	4.0528	380.863
369.999	2.9114	814.738	385.000	3.8723	596.279	395.000	4.3301	381.184
374.999	3.8439	814.202	390.000	4.3482	596.003	400.000	4.6044	381.276
379.999	4.7963	813.674	394.999	4.8378	595.734	379.999	3.0631	194.146
385.000	5.7639	813.196	400.001	5.3367	595.536	390.000	3.3009	194.007
389.999	6.7408	812.684	383.499	3.7101	522.746	400.000	3.5316	193.878
377.999	3.4259	731.555	385.000	3.8257	521.438	359.998	1.4528	69.448
379.998	3.7055	731.379	389.999	4.2194	521.066	379.999	1.5855	69.528
381.998	3.9896	731.203	395.000	4.6207	520.993	400.000	1.7148	69.604

Table A2. Experimental vapor pressures p_{sat} for R1234ze(E);
an average of the replicates at each temperature is given.

T/K	p_{sat}/MPa	T/K	p_{sat}/MPa	T/K	p_{sat}/MPa	T/K	p_{sat}/MPa
filling 1							
274.996	0.2317	309.997	0.7027	324.997	1.0455	355.000	2.0883
279.995	0.2767	314.997	0.8061	329.998	1.1835	360.001	2.3197
284.994	0.3281	317.997	0.8730	334.998	1.3346	365.001	2.5706
289.994	0.3866	318.997	0.8963	339.998	1.4999	370.002	2.8427
294.993	0.4527	319.998	0.9200	344.999	1.6792	375.002	3.1385
299.997	0.5269	320.997	0.9441	349.999	1.8753	380.002	3.4611
304.997	0.6101	321.997	0.9687				
filling 2							
260.998	0.1351	261.997	0.1408	319.995	0.9199	329.995	1.1834